

Observations on the unit-cell dimensions, H₂O contents, and δD values of natural and synthetic alunite

ROGER E. STOFFREGEN*

Department of Geological Sciences, Southern Methodist University, Dallas, Texas 75275, U.S.A.

CHARLES N. ALPERS**

Department of Geological Sciences, McGill University, 3450 University St., Montreal, Quebec H3A 2A7, Canada

ABSTRACT

Unit-cell dimensions for synthetic alunite and natroalunite formed at 450 °C are $a = 6.981(1) \text{ \AA}$, $c = 17.331(4) \text{ \AA}$ and $a = 6.9786(7) \text{ \AA}$, $c = 16.696(3) \text{ \AA}$, respectively. Synthetic alunite-natroalunite solid solutions show a linear variation in c with mole fraction Na, but this trend is obscured in natural samples by heterogeneities in Na content. The mole fraction Na in natural samples can be estimated by $X_{\text{Na}} = (17.331 - c)/0.635$ with an accuracy of ± 0.10 . Alunite from low-temperature environments is characterized by fine grain size ($< 5 \mu\text{m}$), an anomalously large value of a , significant H₂O loss during heating in a vacuum at 300–400 °C, and total H₂O in excess of the stoichiometric value. In contrast, alunite from hydrothermal environments is coarser grained, has an a value identical to synthetic alunite formed at 450 °C, evolves negligible H₂O when heated to 400 °C, and does not contain H₂O in excess of the stoichiometric amount. The value of δD of the H₂O evolved when alunite is heated at 400 °C is shifted toward local meteoric H₂O relative to the bulk H₂O, suggesting that the low-temperature H₂O exchanges with ambient H₂O vapor at room temperature.

INTRODUCTION

Alunite [KAl₃(SO₄)₂(OH)₆] is one of the most abundant minerals in the isostructural alunite-jarosite supergroup (Scott, 1987). Alunite forms between 15 and 400 °C as an alteration product of Al-bearing minerals in relatively oxidizing, S-rich environments. Numerous chemical substitutions are possible in the alunite structure including Fe³⁺ for Al³⁺ (Brophy et al., 1962), PO₄³⁻ or AsO₄³⁻ for SO₄²⁻, and Na⁺, H₃O⁺, Ca²⁺, or Sr²⁺ for K⁺ (Scott, 1987; Stoffregen and Alpers, 1987), but relatively little information is available about the crystallographic effects of these substitutions. This paper is primarily concerned with the substitution of Na⁺ for K⁺, which is the most common chemical variation in alunite, and with the occurrence of H₃O⁺ and other forms of non-OH H₂O in alunite.

The variation in alunite unit-cell dimensions with X_{Na} has been studied both with synthetic and natural alunite samples by Parker (1962) and Cunningham and Hall (1976). However, these studies were limited by a lack of data over the entire compositional range and also by heterogeneity in the Na content of natural specimens, which precludes accurate measurement of unit-cell dimensions. We present data on synthetic alunite samples of inter-

mediate composition that provide more precise unit-cell dimensions and better constraints on alunite-natroalunite mixing volumes than the prior studies. Hydronium (H₃O⁺) substitution is more difficult to document than the Na⁺ substitution but has been inferred in virtually all synthetic alunite because of a deficiency in alkalis and an excess in H₂O contents compared with the stoichiometric composition (e.g., Ripmeester et al., 1986). The nonstoichiometric H₂O is generally attributed to the presence of H₃O⁺ but may also reflect other forms of "excess water" as discussed by Ripmeester et al. (1986). All H₂O in excess of the amount predicted by mineral stoichiometry for the OH site is referred to here as non-OH H₂O. Such H₂O is important because it may complicate interpretation of alunite δD and $\delta^{18}\text{O}$ data, which have been used to study a variety of ore-forming environments by Rye et al. (1992). We have therefore attempted to quantify the concentration of non-OH H₂O in natural alunite from different environments and to determine if its presence can be easily detected by changes in unit-cell dimensions.

ALUNITE SAMPLES USED IN THIS STUDY

Synthetic alunite and natroalunite were precipitated at 150 °C from solutions described by Parker (1962). Two additional alunite samples were prepared by heating the alunite formed at 150 °C in a 0.7-*m* K₂SO₄ solution at 250 °C for 10 d and in a solution of 0.6-*m* K₂SO₄ and 0.65-*m* H₂SO₄ at 450 °C for 5 h. Two additional natroalunite samples were prepared by heating the natroalunite

* Present address: AWK Consulting Engineers, 1225 Rodi Road, Turtle Creek, Pennsylvania 15145, U.S.A.

** Present address: U.S. Geological Survey, Water Resources Division, Room W-2235, Federal Building, 2800 Cottage Way, Sacramento, California 95825, U.S.A.

formed at 150 °C in a 1.0-*m* Na₂SO₄ solution at 250 °C for 10 d and in a solution of 0.6-*m* Na₂SO₄ and 0.65-*m* H₂SO₄ at 450 °C for 5 h. In addition, hydronium alunite was synthesized at 170 °C using the method of Ripmeester et al. (1986). The alunite-natroalunite solid solutions used in this study were prepared in ion-exchange experiments at 450 °C by Stoffregen and Cygan (1990).

We have also studied 38 natural alunite specimens, which can be broadly subdivided into four groups on the basis of their grain size, mode of occurrence, and morphology: disseminated, coarse vein, porcelaneous vein, and fine grained. Disseminated alunite occurs in bladed crystals 1–10 mm in length that replace feldspar grains and are accompanied by quartz and fine disseminated pyrite. Coarse vein alunite occurs in crystals >1 mm in nearly monomineralic veins or pods that may be up to several meters in width. Porcelaneous vein alunite occurs in grains of 5–100 μm with irregular surfaces within veinlets a few millimeters to a few centimeters wide and may be accompanied by minor quartz and kaolinite. Fine-grained alunite occurs in pseudocubic grains 0.5–5 μm in length within veinlets, small concretions, or bedded sediments.

ANALYTICAL METHODS

Powder XRD data were obtained using Cu radiation with a Scintag PAD-V diffractometer operated at 40 kV and 30 mA. Quartz was used as an internal standard for the natural specimens and corundum for the synthetic samples. Unit-cell dimensions obtained on the same sample using the two different internal standards agree to within 1σ. Scans were obtained over a 2θ range of 10–65° at a scan speed of 0.01°/s using zero-background mounts. Hexagonal-rhombohedral unit-cell refinements were obtained with the program Latcon (Scintag, 1987) based on 16–22 reflections for the synthetic samples and 10–18 reflections for the natural specimens.

The Na and K contents of synthetic alunite discussed in this study are from Stoffregen and Cygan (1990). Na and K contents of natural alunite were measured by atomic absorption with a precision of 2%.

Total H₂O was determined by H₂ manometry using a modified version of the alunite H extraction technique of Wasserman et al. (1990) and also by Karl Fischer titration. Samples used for H₂ manometry were ground with a mortar and pestle, and 40–60 mg of the fraction with –325 mesh size were placed in a Mo crucible that was heated overnight under vacuum at 120 °C to remove adsorbed H₂O. After preheating, each sample was heated in a resistance furnace in one or two 1-h steps. The amount of H₂ produced during each step was determined manometrically. This procedure was modified from the step-heating technique used by Alpers et al. (1988) to study jarosite. For most samples, the initial step was at 350 °C and was followed by a second step at 400 °C. Samples thought to contain negligible non-OH H₂O were heated only at 400 °C, and those samples that contained large

amounts of excess H₂O were heated first at 300 °C and then at 350 °C for 1 hr. All samples were then heated for 1 h at approximately 950 °C in either a resistance furnace or an induction heater.

The H₂O evolved at each of these steps was reduced to H₂ using U metal and then transferred with a Toepler pump into a known volume, which had previously been calibrated for pressure as a function of mass using known masses of H₂O sealed in glass capillaries. One blank was processed with each five samples. The precision of the method for total H₂O is 2%. Accuracy was determined using sealed glass capillary tubes containing 5 mg of H₂O and was also within 2%. An independent measure of total H₂O content was obtained by Karl Fischer titration after heating the samples overnight at 110 °C at 1 atm pressure. H₂O contents determined by this method agreed to within 3.5% of the manometric values in seven of the nine samples for which both measurements were made. The δD measurements were made using a Finnigan MAT 251 mass spectrometer. For most samples δD of the H₂O evolved below 400 °C was measured separately from δD of the H₂O evolved at 950 °C. A single δD measurement of the total H₂O was made only on the Summitville, Marysvale, and La Escondida specimens and the natroalunite formed at 450 °C, all of which evolved less than 0.37 wt% H₂O at 400 °C.

XRD RESULTS

Synthetic samples

Published unit-cell dimensions for end-member alunite, natroalunite, and hydronium alunite are shown in Figure 1. The large range in *a* and *c* in this figure is probably the result of non-OH H₂O in some samples. For example, Menchetti and Sabelli (1976) report *c* equal to 17.223 Å for alunite, which is approximately 0.1 Å smaller than most of the other published values. On the basis of their description of the synthesis method used, this almost certainly reflects the presence of non-OH H₂O in their sample. Many of the other studies do not provide information on the H₂O content of their samples (e.g., Wang et al., 1965), and as such their results cannot be assumed to be representative of stoichiometric alunite or natroalunite.

These data can be compared with results obtained for our synthetic samples (Table 1, Fig. 1). Unit-cell dimensions for the synthetic end-member alunites formed at 250 and 450 °C agree within 2σ for *c* and *a*, whereas the sample formed at 150 °C has significantly larger *a* and smaller *c* and *V*. These results are similar to data from Parker (1962) for synthetic alunite formed at 100 °C, which showed an increase in *c* and a decrease in *a* after heating in air for 1 h at 300 °C. Parker attributed this shift in unit-cell dimensions to the loss of non-OH (hydronium) H₂O during heating. This is confirmed for our samples by a decrease in H₂O content from 128% of the amount predicted for stoichiometric alunite in the sample formed at 150 °C to about 105% of this amount in the other two

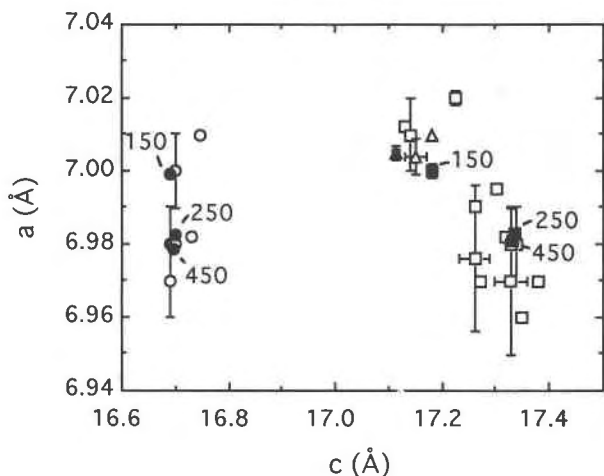


Fig. 1. Unit-cell dimensions from previous studies for alunite (open squares), natroalunite (open circles), and hydronium alunite (open triangles) and from this study for alunite (solid squares), natroalunite (solid circles), and hydronium alunite (solid triangle). Formation temperatures (in degrees Celsius) for alunite and natroalunite from this study are also shown. Error bars represent reported standard deviations. Sources of data are Hendricks (1937), Pabst (1947), Parker (1962), Brophy et al. (1962), Wang et al. (1965), Kashkay (1969), Kubisz (1964, 1970), Menchetti and Sabelli (1976), Giuseppetti and Tadini (1980), Ossaka et al. (1982), Aoki (1983), and Ripmeester et al. (1986).

synthetic alunite samples (Table 1). Similarly, the natroalunite formed at 150 °C has a significantly larger value of a than the natroalunite samples formed at 250 and 450 °C and also contains the most H₂O of the three.

Also shown in Figure 1 are unit-cell data for synthetic hydronium alunite prepared following the method of Ripmeester et al. (1986). The value of c for hydronium alunite is intermediate between those of alunite and natroalunite, whereas a for hydronium alunite [7.005(2) Å] is significantly larger than the range of 6.978–6.983 Å obtained for the alunite and natroalunite formed at 250 and 450 °C but is similar to the values observed for both samples formed at 150 °C. This suggests that the presence of significant non-OH H₂O in alunite can be recognized by an anomalously large value of a , which should be apparent regardless of the Na content of the sample.

Unit-cell dimensions for 17 synthetic (450 °C) alunite samples of intermediate composition are plotted as a function of composition in Figure 2 along with the samples of end-member alunite and natroalunite formed at 450 °C. The variation in a across this binary is approximately the same size as the average 2σ for a and is thus not significant. Most values of c and V plot on the ideal mixing lines connecting the alunite and natroalunite formed at 450 °C, which have the equations

$$X_{\text{Na}} = (17.331 - c_{\text{meas}})/0.635 \quad (1)$$

and

$$X_{\text{Na}} = (731.5 - V_{\text{meas}})/27.3. \quad (2)$$

TABLE 1. Unit-cell data for synthetic end-member alunite, natroalunite, and hydronium alunite

	a (Å)	c (Å)	V (Å ³)	w/s*
Alunite (150 °C)	7.000(2)	17.180(7)	729.1(4)	128.2
Alunite (250 °C)	6.9831(5)	17.334(2)	732.03(9)	103.9
Alunite (450 °C)	6.981(1)	17.331(4)	731.5(2)	105.5
Natroalunite (150 °C)	6.9990(8)	16.690(3)	708.0(2)	119.6
Natroalunite (250 °C)	6.9823(5)	16.700(2)	705.1(1)	113.0
Natroalunite (450 °C)	6.9786(7)	16.696(3)	704.2(2)	99.1
Hydronium alunite	7.005(2)	17.114(7)	727.2(4)	nd

Note: nd = not determined.

* Equal to $100 \times (\text{measured H}_2\text{O content})/(\text{stoichiometric H}_2\text{O content})$ (see Table 3).

When the uncertainty in the end-member values is also considered, all but four of the samples are within 2σ of ideal mixing. These samples do not define a systematic departure from ideal mixing and are believed to reflect errors in X_{Na} caused by compositional heterogeneity.

Natural alunite

Unit-cell data for natural alunite are presented in Figure 3 and Table 2.¹ Values of a show no systematic variation with X_{Na} , but most of the fine-grained and porcelaneous vein alunite samples have larger a than the other natural specimens and the synthetic samples formed at 450 °C. These anomalously high a values may reflect the presence of non-OH H₂O or substitution of Fe³⁺ for Al³⁺, which also causes an increase in a (Brophy et al., 1962). V and c decrease with increasing Na content, but both show a large amount of scatter. This scatter and the relatively large uncertainties in unit-cell dimensions for many of the natural specimens result from compositional heterogeneity and consequent peak broadening. In spite of these uncertainties, the unit-cell data and Equation 1 provide an estimate of the bulk X_{Na} that is accurate to ± 0.10 for most specimens.

The XRD data indicate that four of the natural specimens are mixtures of two alunites with different X_{Na} . The bulk X_{Na} for these specimens is between 0.40 and 0.70, but the unit-cell data indicate that three of the four are mixtures of relatively pure alunite and natroalunite. In the fourth sample, from Summitville, Colorado, alunites with X_{Na} of 0.68 and 0.23 were identified from the XRD data. It is interesting to note that coarse vein alunite from Komatsuga, Japan, and disseminated alunite from Goldfield, Nevada, are the only specimens studied, besides the Summitville alunite with $X_{\text{Na}} = 0.68$, that are within the range of $X_{\text{Na}} = 0.40$ and 0.70 on the basis of Equation 1. The absence of fine-grained and porcelaneous vein alunite in this range may reflect a miscibility gap between alunite and natroalunite, a possibility also suggested by the experimental data of Stoffregen and Cygan (1990).

¹ A copy of Table 2 may be ordered as Document AM-92-504 from the Business Office, Mineralogical Society of America, 1130 Seventeenth Street NW, Suite 330, Washington, DC 20036, U.S.A. Please remit \$5.00 in advance for the microfiche.

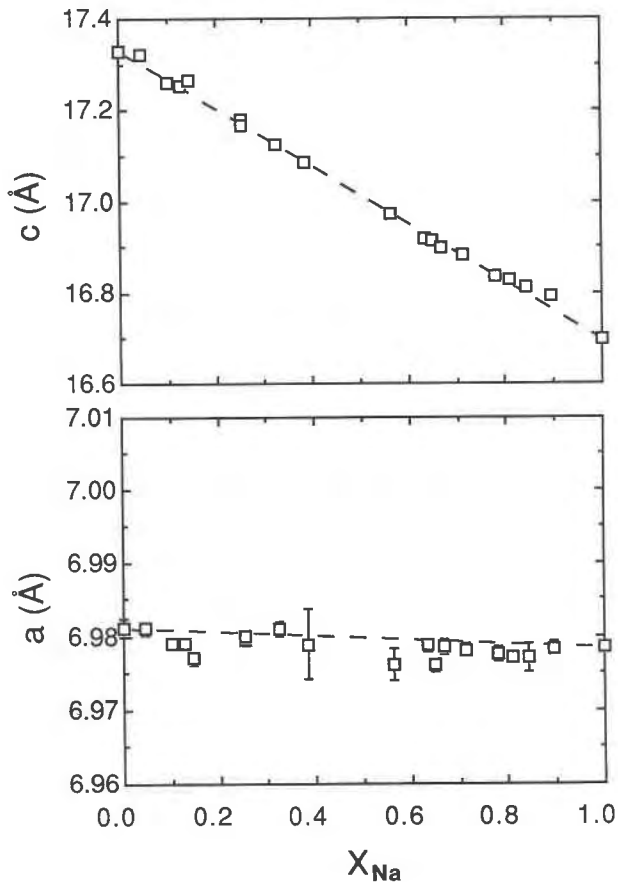


Fig. 2. Unit-cell dimensions of synthetic alunite-natroalunite solid solutions formed at 450 °C plotted against composition [X_{Na} = molar ratio $\text{Na}/(\text{Na} + \text{K})$]. Dashed lines connect end-member values (Table 1). Errors (1σ) are less than the symbol size except where shown.

H₂O CONTENT

Previous work

Non-OH H₂O has been well documented in synthetic alunite (Fielding, 1980; Ripmeester et al., 1986) and has also been reported in fine-grained natural alunite. The presence of this H₂O is generally inferred on the basis of H₂O contents, obtained by difference, that are greater than the predicted values for stoichiometric alunite (13.05 wt% H₂O) and natroalunite (13.58 wt% H₂O). These high H₂O contents are generally attributed to the presence of hydronium (H₃O⁺), but a second type of H₂O referred to as nonstoichiometric water by Ripmeester et al. (1986) may be present in the form of H bonded either to OH or sulfate O atoms to resolve the charge imbalance due to Al deficiency in some alunite (Härtig et al., 1984; Ripmeester et al., 1986; Bohmhammel et al., 1987). A third type of H₂O was defined by Ripmeester et al. (1986) as excess water, in reference to the quantity of H₂O from the chemical analysis (either by difference or direct methods) that cannot be accommodated on any of the crystallographic sites postulated for H: OH, H₃O⁺, or nonstoi-

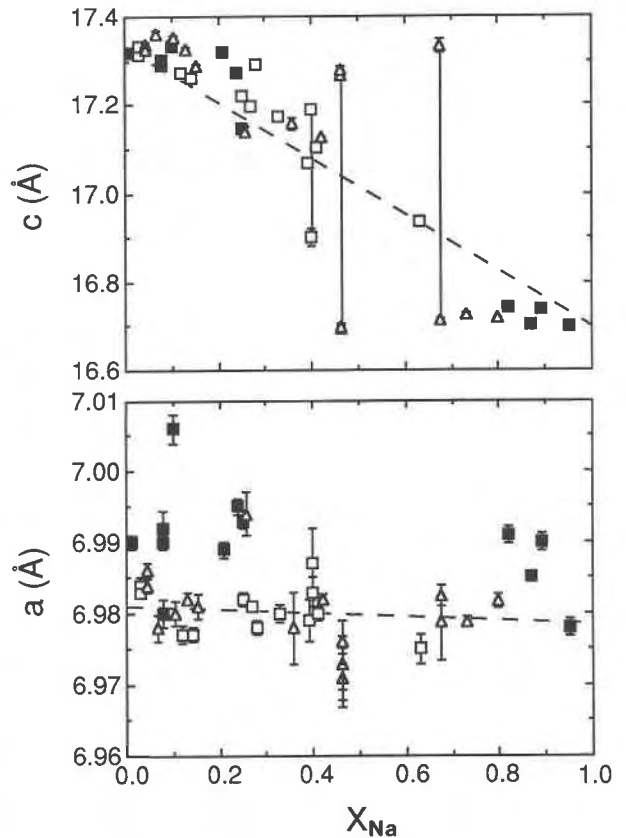


Fig. 3. Unit-cell dimensions of 38 natural alunite specimens plotted against composition. Open squares are disseminated and coarse vein alunite, solid squares are porcelaneous vein and fine-grained alunite, and open triangles are unclassified. Vertical lines connect alunite pairs from the same specimen. Dashed lines connect values for synthetic end-members as in Figure 2. Errors (1σ) are less than the symbol size except where shown.

chiometric H. Assignment of H₂O to these different sites requires compositional data on sulfate and Al in alunite which were not obtained in this study. As a result, we have not attempted to assign the non-OH H₂O to specific crystallographic sites.

Non-OH H₂O may be distinguished by the decomposition behavior of alunite as a function of temperature. OH H₂O in alunite is released over a temperature range of 500–600 °C during thermogravimetric analysis (e.g., Kashkay and Babaev, 1969). In contrast, synthetically prepared alunite invariably yields some H₂O over the temperature range of 300–400 °C (e.g., Fielding, 1980; Pysiak and Glinka, 1981), and this weakly held H₂O is generally thought to correspond to the total non-OH H₂O present. To characterize the non-OH H₂O in natural and synthetic alunite better, we have measured both the total H₂O content and the amount of H₂O evolved during heating in a vacuum at 300–400 °C.

Results

H₂O contents of six synthetic and eight natural alunite samples are given in Table 3. The amount of H₂O evolved

TABLE 3. H₂O evolved during heating of alunite under vacuum

	Wt% H ₂ O evolved					Total*	Total**	Stoichiometric wt% H ₂ O†	w/s‡	δD low§	δD high
	300 °C	350 °C	400 °C	950 °C	Total*						
Alunite (150 °C)	5.69	0.76		10.27	16.72	16.64	13.05	128.2	-68	-64	
Alunite (250 °C)		0.89	0.99	11.68	13.56	13.63	13.05	103.9			
Alunite (450 °C)			1.59	12.18	13.77		13.05	105.5			
Natroalunite (150 °C)	1.46	0.85		13.93	16.24	16.00	13.58	119.6	-55	-66	
Natroalunite (250 °C)		1.91	0.88	12.56	15.35		13.58	113.0	-69	-63	
Natroalunite (450 °C)			0.09	13.37	13.46		13.58	99.1			
Summitville, Col. (diss.)			0.20			12.91	13.25	97.4			
Marysvale, Utah (cv)			0.32	12.39	12.71	12.91	13.06	97.3	-69	-77	
La Escondida, Chile (cv)			0.36	12.16	12.52	12.44	13.21	94.8		-51	
Mantos Blancos, Chile (pv)		0.21	0.31	12.96	13.48	12.81	13.51	99.8	-40	11	
Round Mountain, Nev. (pv)		0.22	0.16	12.61	12.99	12.55	13.05	99.6	-68	-104	
Death Valley, Cal. (fg)		0.69	0.71	12.75	14.15	14.50	13.50	104.8	-56	-77	
Noarlunga, Australia (fg)		0.44	0.41	13.59	14.44		13.08	110.4	-31	-14	
Sadler, Tex. (fg)	0.99	0.51		12.79	14.29	15.30	13.47	106.1	-22	-20	

Note: diss. = disseminated; cv = coarse vein; pv = porcelaneous vein; fg = fine grained.

* Total H₂O as determined by H₂ manometry.

** Total H₂O as determined by Karl Fischer titration.

† Stoichiometric H₂O content based on the measured X_{Na}.

‡ Equal to 100 × (measured wt% H₂O)/(stoichiometric wt% H₂O). Where available, the manometric value for measured wt% H₂O is used.

§ The δD of H₂O evolved at or below 400 °C.

|| Equal to bulk δD where no low-temperature δD is given, otherwise equal to δD for H₂O evolved at 950 °C.

by the synthetic samples during low temperature heating ranged from 5.69 wt% at 300 °C for the alunite formed at 150 °C to 0.09 wt% for the natroalunite formed at 450 °C. Values of w/s, which is 100 times the total wt% H₂O measured for the sample divided by the wt% H₂O computed for stoichiometric alunite of the appropriate X_{Na}, ranged from 128.2 to 99.1% for these samples. Except for the fine-grained alunite samples, all of the natural specimens evolved less than 0.6 wt% H₂O during heating below 400 °C and contained between 94 and 100% of the predicted H₂O content. The two examples of porcelaneous alunite, a Na-rich specimen from Mantos Blancos, Chile, and pure potassium alunite from Round Mountain, Nevada, contained 99.8 and 99.6% w/s, respectively. The somewhat lower values of w/s for the Summitville, Marysvale, and La Escondida specimens may reflect the presence of minor quartz or other contaminants. In contrast, the three fine-grained alunites evolved from 0.8 to 1.5 wt% H₂O during low-temperature heating, and all had w/s values greater than 104%.

Although alunite that contains non-OH H₂O yields relatively large amounts of H₂O when heated at 300–400 °C, the amount evolved does not necessarily equal the amount of non-OH H₂O inferred to be present from the total H₂O determination. This is illustrated in Figure 4, which shows the amount of H₂O evolved at or below 400 °C vs. w/s. A sample that released all of its non-OH H₂O but no OH H₂O during low-temperature heating should plot on the reference line in Figure 4. Most of the synthetic and natural samples plot above this line, which suggests that loss of non-OH H₂O is generally accompanied by removal of some OH H₂O. Although it might be possible to optimize the time and temperature of heating to obtain a better separation of non-OH from OH H₂O, our results suggest that the optimal conditions for such a separation might be highly sample dependent.

Values of δD

Although the low-temperature H₂O fraction cannot be equated directly with non-OH H₂O its δD value was measured separately from the δD of H₂O evolved at 950 °C. In Figure 5, the difference between the high- and low-temperature fraction (Δ) is plotted against δD of the high-temperature fraction. This figure also includes four data points for Sadler natroalunite used in isotope exchange experiments from Stoffregen et al. (in preparation). The data define a linear trend with a slope of about 0.7 and a y intercept of 24‰ (R² = 0.89). This pattern demonstrates that the high- and low-temperature δD values are not related by an equilibrium D fractionation factor, which would give a constant Δ value in Figure 5. They also cannot be explained by a Rayleigh fractionation process in which lighter isotopes are preferentially removed during the lower temperature steps, as described by Kuroda et al. (1988) for hornblende and micas.

The pattern in Figure 5 is interpreted to reflect exchange of D between the H₂O evolved at or below 400 °C and ambient H₂O vapor. This process can be described with the equation

$$\delta D_{\text{low}} = (\delta D_{\text{high}})(1 - f) + (\delta D_{\text{eq}})f \quad (3)$$

where δD_{eq} is the equilibrium δD value with respect to ambient H₂O vapor at 25 °C and f is the fraction of H in the low-temperature H₂O that undergoes exchange. This equation assumes that the low-temperature fraction had an initial δD equal to the high-temperature fraction. Rearranging terms gives

$$\Delta = (\delta D_{\text{high}})f - (\delta D_{\text{eq}})f \quad (4)$$

where Δ is equal to δD_{high} - δD_{low}, the value on the ordinate in Figure 5. The slope of the line in Figure 5 (0.7) can be equated with f in Equation 4, and the y-intercept

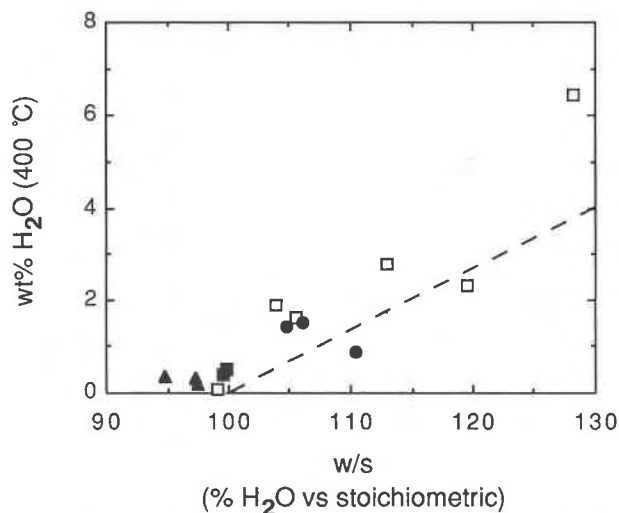


Fig. 4. H_2O evolved at or below 400°C plotted against w/s (Table 3). Dashed line gives the wt% non-OH H_2O for alunite with a given w/s . Open squares are synthetic alunite, solid triangles are disseminated and coarse vein alunite, solid squares are porcelaneous vein alunite, and solid circles are fine-grained alunite.

of 24‰ with $-(\delta D_{\text{ca}})f$, which gives δD_{ca} of -34‰ . This compares with a local H_2O δD of -30 to -40‰ in Dallas, Texas, and suggests a fractionation factor (expressed as $10^3 \ln \alpha$) between the low-temperature H_2O , presumably made up mainly of non-OH H_2O , and ambient H_2O of 0 ± 5 .

The amount of isotopic exchange should be a function of the time during which alunite was exposed to the ambient H_2O vapor, that is, the length of time after it had been brought to Dallas prior to δD analysis. This interval ranged from only a few days to roughly a year. The linear trend on Figure 5 suggests that about two-thirds of the low-temperature H_2O is subject to rapid D-H exchange, perhaps in hours or even minutes, whereas the remaining low-temperature H_2O undergoes minimal exchange at least on a scale of months. Such rapid D-H exchange has also been inferred for surface-correlated H_2O in fine-grained volcanic glasses, as discussed by Newman et al. (1986).

These observations suggest that the H_2O evolved above 400°C will provide a more accurate measure of the initial δD in fine-grained alunite than does the bulk H_2O . Because the amount of low-temperature H_2O in such alunite can exceed 10% of the total H_2O , changes in δD related to exchange with ambient H_2O vapor may have a significant effect on the bulk H_2O δD , particularly if δD for either the sample or the ambient H_2O vapor is extreme. This exchange should not occur with more coarse-grained alunite because it does not contain non-OH H_2O .

DISCUSSION

The observed variation in alunite grain size is believed to be mainly a function of temperature. Fine-grained al-

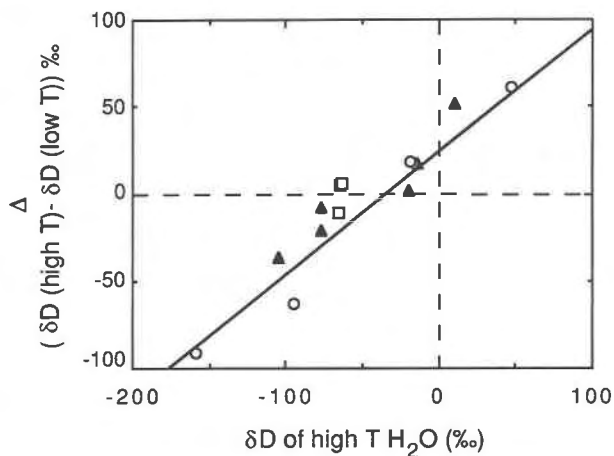


Fig. 5. Values of Δ (difference between δD of H_2O evolved at high and low temperature) plotted against δD for high-temperature H_2O from synthetic and natural alunite. Open squares are synthetic alunite, open circles are experiments from Stoffregen et al. (in preparation), and solid triangles are natural alunite.

unite appears to be limited to near-surface environments. This type of alunite has been reported from weathering profiles (e.g., Meyer and Peña Dos Reis, 1985), intertidal marine environments (e.g., Khalaf, 1990), and lacustrine environments (e.g., Alpers et al., 1992). Porcelaneous vein alunite may form at low temperature, as illustrated by the alunite from Round Mountain, Nevada, which has been interpreted as supergene by Fifarek and Gerike (1991) and Rye et al. (1992). It also forms in modern hot springs, as illustrated by a specimen from the Waiotapu geothermal field included in the data set shown in Figure 3. These two occurrences suggest a range of formation temperatures of 25 to at least 100°C for porcelaneous vein alunite. Disseminated alunite forms at 200 – 300°C , as determined by isotope geothermometry and corroborative geological evidence (Rye et al., 1992). Formation temperatures for coarse vein alunite are not well constrained, although they are likely to be similar to those of disseminated alunite based on the common spatial association of the two alunite types.

Most fine-grained alunite described to date, including the three specimens from this report, contain between 14 and 16 wt% H_2O . This corresponds to between 5 and 35 mol% H_3O^+ on the alkali site if all non-OH H_2O is assumed to be present as H_3O^+ . More H_3O^+ -rich fine-grained alunites, including a pure hydronium alunite (Khalaf, 1990), have also been reported. The common occurrence of non-OH H_2O in fine-grained alunite suggests that at near-surface temperatures, fluid $[\text{H}_3\text{O}^+ / (\text{Na} + \text{K})]$ ratios are generally large enough to stabilize some H_3O^+ component in alunite. Some alunite from modern geothermal areas also contains H_3O^+ (e.g., Aoki, 1983), which suggests that a H_3O^+ component may be stable at least up to 100°C . This is consistent with the presence of non-OH H_2O in synthetic alunite and natroalunite formed at 150°C . However, the non-OH H_2O in these and the fine-

grained natural alunite may also be a nonequilibrium effect and does not prove that a H_3O^+ component is stable in alunite at any temperature. The absence of non-OH H_2O in disseminated alunite, as indicated by our H_2O determinations and by the lack of the anomalous a values, strongly suggests that a hydronium-alunite component is not stable above 200 °C. This is consistent with the observed decrease in H_2O content of synthetic alunite and natroalunite formed at 150 °C when heated to 250 and 450 °C.

ACKNOWLEDGMENTS

We thank Michael Bird, Ed Bloomstein, Gerhard Beukes, Bill Chavez, Skip Cunningham, Mary Gilzean, Eiji Izawa, David John, Curtis Kortemeier, Patty Murtha, Malcolm Ross, and Stuart Simmons for specimens used in this study. Mike Colucci, Kurt Ferguson, and the late Jim Borthwick assisted with the H extractions and made δD measurements. This work was supported in part by NSF grants EAR-8816706 (R.E.S.) and EAR-9005536 (R.E.S.) and by the Water Resources Division of the U.S. Geological Survey in cooperation with Kirk Nordstrom. XRD data were acquired on a Scintag diffractometer obtained with NSF grant EAR-8721093 to M.J. Holdaway. A portion of the work was completed while one of us (C.N.A.) was a National Research Council Resident Research Associate with the U.S. Geological Survey. Helpful reviews of the manuscript were provided by J.M. Hughes, K. Scott, and an anonymous referee.

REFERENCES CITED

- Alpers, C.N., Nordstrom, D.K., and White, L.D. (1988) Solubility and deuterium fractionation factor for hydronium-bearing jarosites precipitated from acid mine waters. *Eos*, 69, 1480–1481.
- Alpers, C.N., Rye, R.O., Nordstrom, D.K., White, L.D., and King, B.S. (1992) Chemical, crystallographic, and isotopic properties of alunite and jarosite from acid-hypersaline Australian lakes. *Chemical Geology*, 96, 203–226.
- Aoki, M. (1983) Modes of occurrence and mineralogical properties of alunite solid solution in Osorezan geothermal area. *Sciences Report of Hirosake University*, 30, 132–141 (in Japanese).
- Bohmhammel, K., Naumann, R., and Paulik, F. (1987) Thermoanalytical and calorimetric investigations on the formation and decomposition of some alunites. *Thermochimica Acta*, 121, 109–119.
- Brophy, G.P., Scott, E.S., and Snellgrove, R.A. (1962) Sulfate studies II. Solid solution between alunite and jarosite. *American Mineralogist*, 47, 112–126.
- Cunningham, C.G., and Hall, R.B. (1976) Field and laboratory tests for the detection of alunite and determination of atomic percent potassium. *Economic Geology*, 71, 1596–1598.
- Fielding, S.J. (1980) Crystal chemistry of the oxonium alunite–potassium alunite series. M.S. thesis, Lehigh University, Bethlehem, Pennsylvania.
- Fifarek, R.H., and Gerike, G.N. (1991) Oxidation of hydrothermal sulfides at Round Mountain, Nevada—origin and relation to gold mineralization. In G.L. Raines, R.E. Lisle, R.W. Schafer, and W.H. Wilkinson, Eds., *Geology and ore deposits of the great basin: Symposium proceedings*, p. 1111–1121. Geological Society of Nevada, Reno, Nevada.
- Giuseppetti, G., and Tadani, C. (1980) The crystal structure of osarizawaite. *Neues Jahrbuch für Mineralogie Monatshefte*, 401–407.
- Härtig, C., Brand, P., and Bohmhammel, K. (1984) Fe-Al Isomorphie und Strukturwasser in Kristallen von Jarosit-Alunit-Typ. *Zeitschrift für anorganische und allgemeine Chemie*, 508, 159–164.
- Hendricks, S.B. (1937) The crystal structure of alunite and the jarosites. *American Mineralogist*, 22, 773–785.
- Kashkay, C.M. (1969) Alunite group and its structural analogs. *Vsesoiuznoe Mineralogicheskoe Obshchestvo Zapiski*, 98, 150–165 (in Russian).
- Kashday, M.A., and Babaev, I.A. (1969) Thermal investigations on alunite and its mixtures with quartz and dickite. *Mineralogical Magazine*, 37, 128–134.
- Khalaf, F.I. (1980) Diagenetic alunite in clastic sequences, Kuwait, Arabian Gulf. *Sedimentology*, 37, 155–164.
- Kubisz, J. (1964) A study of minerals of the alunite-jarosite group. *Polska Akademia Nauk Prace Geologiczne*, 22, 1–93 (in Polish, with English summary).
- (1970) Studies on synthetic alkali-hydronium jarosites. I. Synthesis of jarosite and natrojarosite. *Mineralogia Polonica*, 1, 45–57.
- Kuroda, Y., Matsuo, S., and Yamada, T. (1988) D/H fractionation during dehydration of hornblende, mica and volcanic glass. *Journal of Mineralogy, Petrology, and Economic Geology*, 83, 95–101.
- Menchetti, S., and Sabelli, C. (1976) Crystal chemistry of the alunite series: Crystal structure refinement of alunite and synthetic jarosite. *Neues Jahrbuch für Mineralogie Monatshefte*, 406–417.
- Meyer, R., and Peña Dos Reis, R.B. (1985) Paleosols and alunite silcretes in continental Cenozoic of western Portugal. *Journal of Sedimentary Petrology*, 55, 76–85.
- Newman, S., Stolper, E.M., and Epstein, S. (1986) Measurement of water in rhyolitic glasses: Calibration of an infrared spectroscopic technique. *American Mineralogist*, 71, 1527–1541.
- Ossaka, J., Hirabayashi, J., Okada, K., and Harada, J. (1982) Crystal data for $3\text{Al}_2\text{O}_3 \cdot 4\text{SO}_3 \cdot 8\text{H}_2\text{O}$. *Journal of Applied Crystallography*, 15, 353–354.
- Pabst, A. (1947) Some computations on svanbergite, woodhouseite, and alunite. *American Mineralogist*, 32, 16–30.
- Parker, R. (1962) Isomorphous substitution in natural and synthetic alunite. *American Mineralogist*, 47, 127–136.
- Pysiak, J., and Glinka, A. (1981) Thermal decomposition of basic aluminum potassium sulphate. Part I. Stages of decomposition. *Thermochimica Acta*, 44, 21–28.
- Ripmeester, J.A., Ratcliffe, C.I., Dutrizac, J.E., and Jambor, J.L. (1986) Hydronium ion in the alunite-jarosite group. *Canadian Mineralogist*, 24, 435–447.
- Rye, R.O., Bethke, P.M., and Wasserman, M.D. (1992) The stable isotope geochemistry of acid sulfate alteration. *Economic Geology*, 87, 225–262.
- Schoch, A.E., Beukes, G.J., Van der Westhuizen, W.A., and de Bruijn, H. (1989) Natroalunite from Koenabib, Pofadder district, South Africa. *South African Journal of Geology*, 92, 20–28.
- Scintag (1987) PAD V diffraction system users manual (revision 1.0). Scintag, Inc., Santa Clara, California.
- Scott, K. (1987) Solid solution in, and classification of, gossan-derived members of the alunite-jarosite family, northwest Queensland, Australia. *American Mineralogist*, 72, 178–187.
- Stoffregen, R.E., and Alpers, C.N. (1987) Woodhouseite and svanbergite in hydrothermal ore deposits: Products of apatite destruction during advanced argillic alteration. *Canadian Mineralogist*, 25, 201–211.
- Stoffregen, R.E., and Cygan, G.L. (1990) An experimental study of Na-K exchange between alunite and aqueous sulfate solutions. *American Mineralogist*, 75, 209–220.
- Wang, R., Bradley, W.F., and Steinfink, H. (1965) The crystal structure of alunite. *Acta Crystallographica*, 18, 249–252.
- Wasserman, M.D., Rye, R.O., Bethke, P.M., and Arribas, A. (1990) Methods for separation of alunite from associated minerals and subsequent analysis of D, ^{18}O -OH, ^{18}O - SO_4 , and ^{34}S . *Geological Society of America Abstracts with Programs*, 22, A135.

MANUSCRIPT RECEIVED JUNE 3, 1991

MANUSCRIPT ACCEPTED MAY 20, 1992